Supporting Information

Carbon quantum dots capped with metal ion for efficient optical optoelectronic applications

Yuanyuan Han, Weihua Li, Jishuai Lin, Haiguang Zhao, Xiaohan Wang*, Yuanming Zhang**

College of Textiles and Clothes, State Key Laboratory of Bio-Fibers and Eco-Textiles, College of Physics, University Industry Joint Center for Ocean Observation and Broadband Communication, Qingdao University, No. 308 Ningxia Road, Qingdao 266071, P.R. China

* Corresponding author. College of Textiles and Clothes, State Key Laboratory of Bio-Fibers and Eco-Textiles, College of Physics, University Industry Joint Center for Ocean Observation and Broadband Communication, Qingdao University, No. 308 Ningxia Road, Qingdao 266071, P.R. China

E-mail address: xh_wang@qdu.edu.cn (*X Wang*), hgzhao@qdu.edu.cn (*H Zhao*) zhangyuanming001@163.com (*Y Zhang*)

1. Characterizations

The Transmission electron microscopy (TEM) and the high-resolution transmission electron microscopy (HRTEM)of the C-dots was characterized using a JEOL 2100F TEM with a magnification of 10 nm and 2 nm to observe the C-dots. A Thermo Scientific K-Alpha photoelectron spectrometer was used to measure the X-ray photoelectron spectra (XPS) of the C-dots. The Fourier transform infrared (FT-IR) was performed on a Nicolet 6700 FT-IR spectrometer. The UV-Vis spectra and the fluorescence spectra of the C-dots was measured by Lambda 750 UV/Vis spectrometer and Edinburgh FLS1000 instrument. The fluorescence lifetime of C-dots was tested by fluorescence spectrometer. The QYs of the as-prepared C-dots were measured using Edinburgh FLS1000 fluorescence spectrophotometer equipped with integrating sphere. The QYs of the C-dots were determined by selecting the excitation wavelength at 375 nm and the emission range from 350 to 700 nm. The Al-C-dots was pumped with a wavelength of 365 nm with the decay time ranging from 300 fs to 1 ns.

For the LSC measurements, one edge of the LSC was fully covered by the commercial solar cells (PCE: 15%). The external optical efficiency and PCE of the LSC was measured at

Qingdao City, China. We chose the noon for the measurement with the light intensity of 50 mW/cm^2, which was directly measured by using a commercial calibrated Zolix QE-B1 solar cell. As the LSC is symmetrical, we can reasonably assume that the output fluorescent intensity at each edge is same. The external optical efficiency was measured by directly attached a power meter (Newport 843-R) on the edges of the LSC. For the PCE measurement, the measured current intensity was used to calculate the PCE of the LSC by using the equation of PCE = $4\times(J_{sc}\times V_{oc}\times FF)/(P_{in}\times G)\times 100\%$. The geometric factor (G) was defined as the ratio of surface area and edge area (L/4d), where L is length of the LSC and d is the overall thickness of the LSC. In this study, the G factor is calculated as 4.7. The photostability of the LSC was measured by home-made set-up. The UV light with intensity of 100 mW/cm^2, was used to excite the LSC and the detector was put on the edge of the LSC in ambient conditions (25 ℃, 40% humidity).

2. Figures

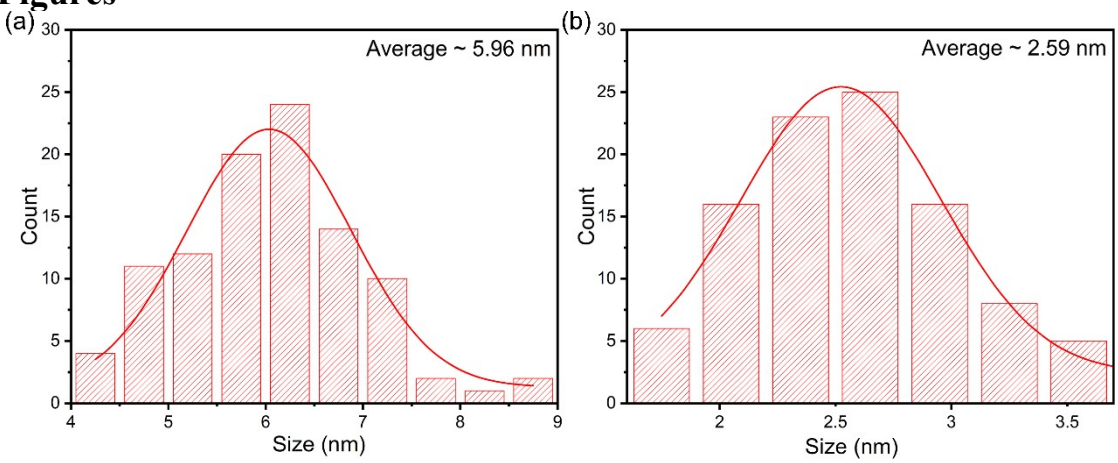

Figure S1. Particle size distributions of the C-dots (Al^{3+}) (a) and C-dots (Mn^{2+}) (b).

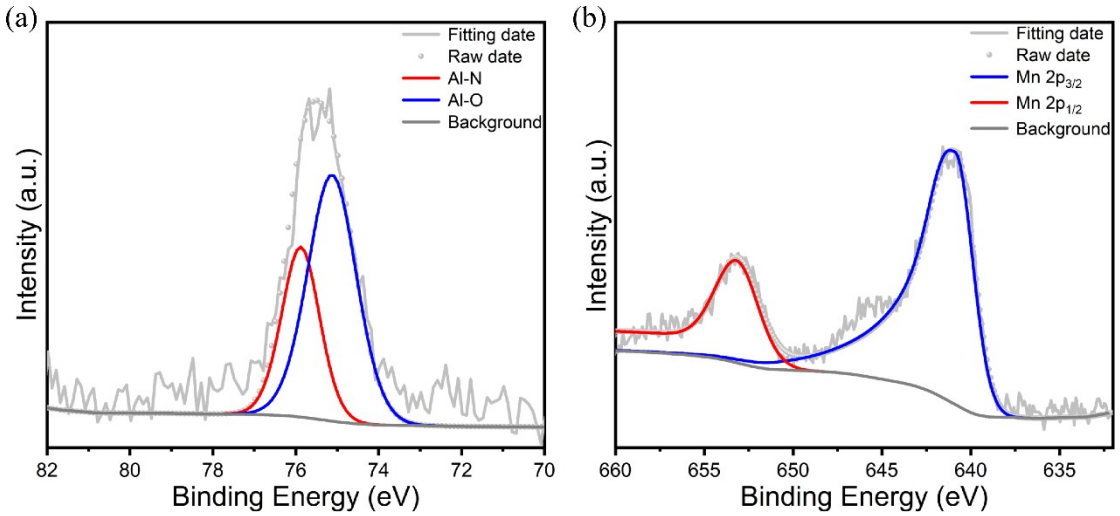

Figure S2. High resolution XPS spectra of (a) Al 2p of the C-dots (Al^{3+}) and (b) Mn 2p of the C-dots (Mn^{2+}).

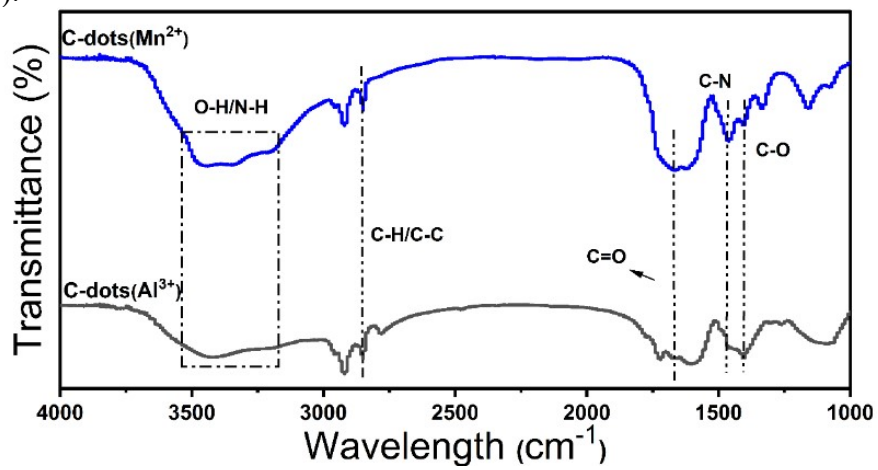

Figure S3. FTIR of the C-dots (Al^{3+}) and C-dots (Mn^{2+}).

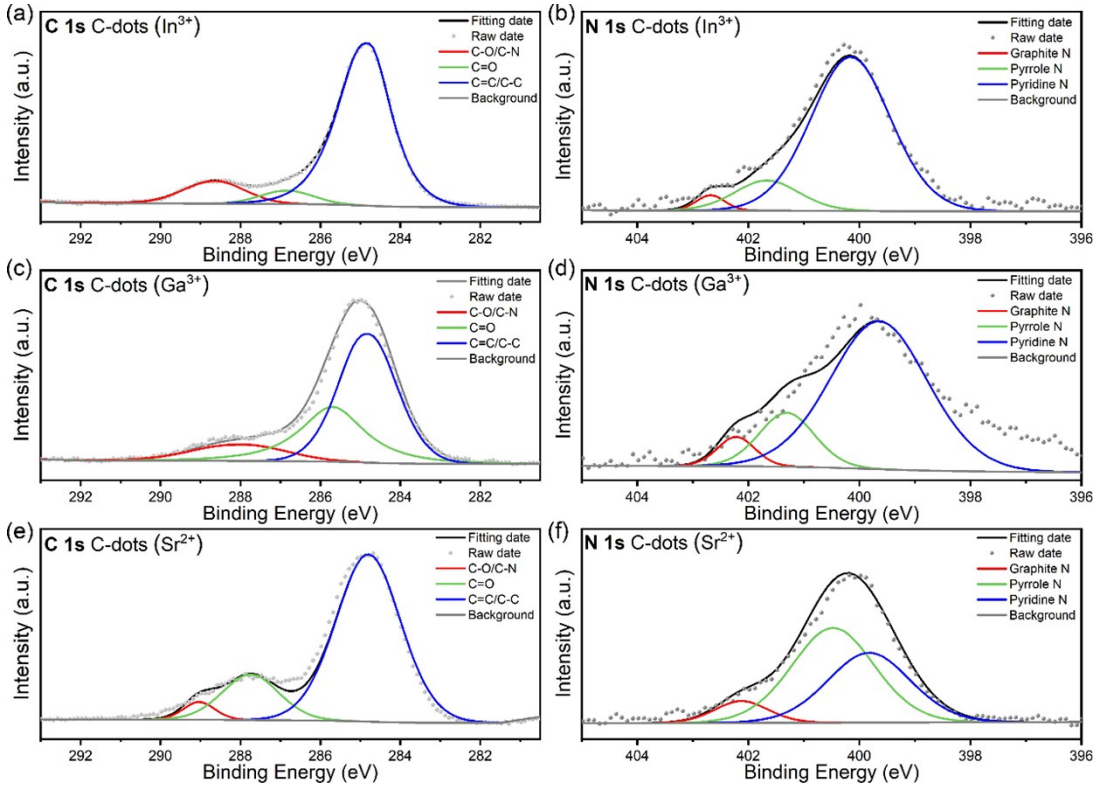

Figure S4. High resolution XPS of C 1s (a), N 1s (b) spectra of the C-dots (In^{3+}); high resolution XPS C 1s (c), N 1s (d) spectra of the C-dots (Ga^{3+}) and high resolution XPS of C 1s (e), N 1s (f) spectra of the C-dots (Sr^{2+}).

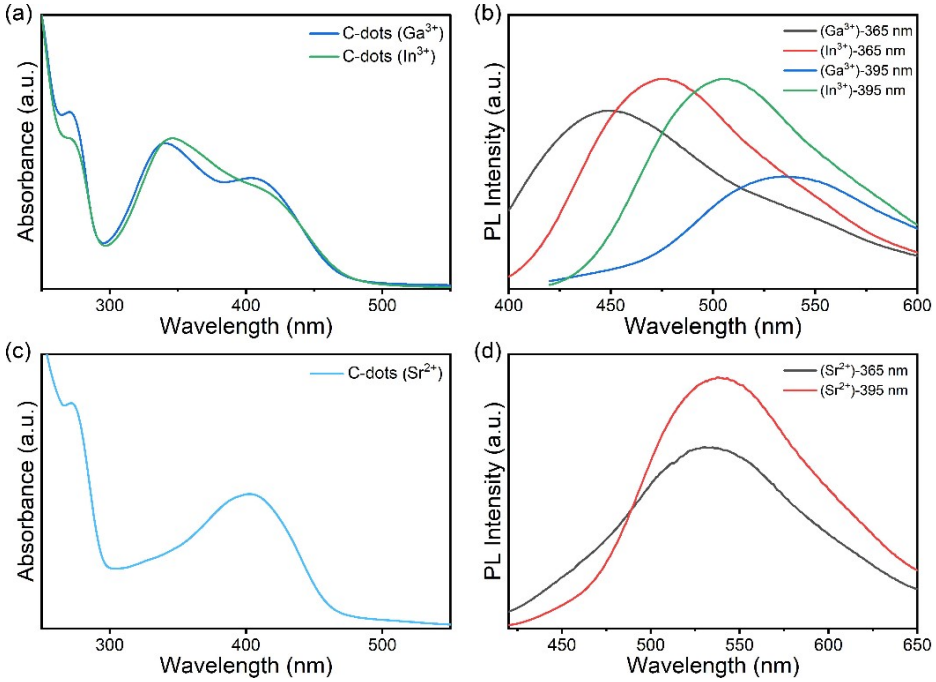

Figure S5. Absorption (a) and fluorescence (b) spectra of the C-dots (Ga^{3+}) and C-dots (In^{3+}). Absorption (c) and fluorescence (d) spectra of the C-dots (Sr^{2+}).

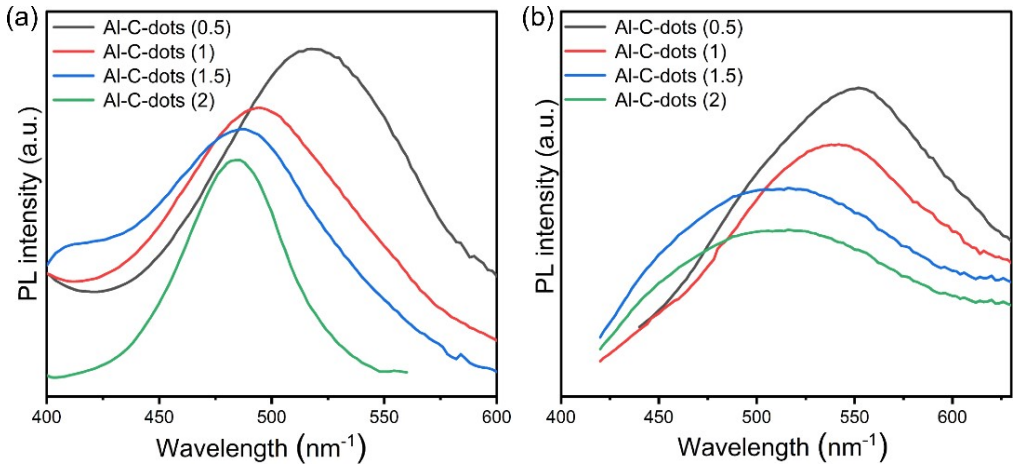

Figure S6. PL spectra of the C-dots (Al^{3+}), the contents of the Al^{3+} were 0.5 g,1 g, 1.5 g and 2 g, respectively. The wavelength was at 365 nm (a) or 395 nm (b).

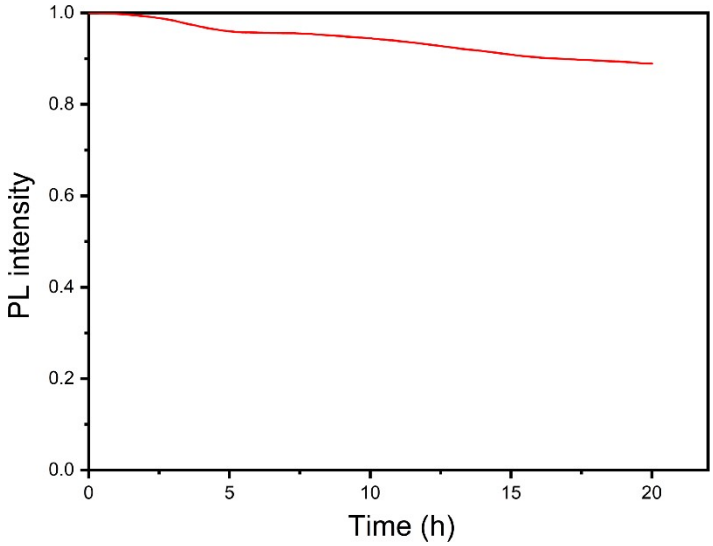

Figure S7. Fluorescence intensity of Al-C-dots in 20 hours continuous illumination.

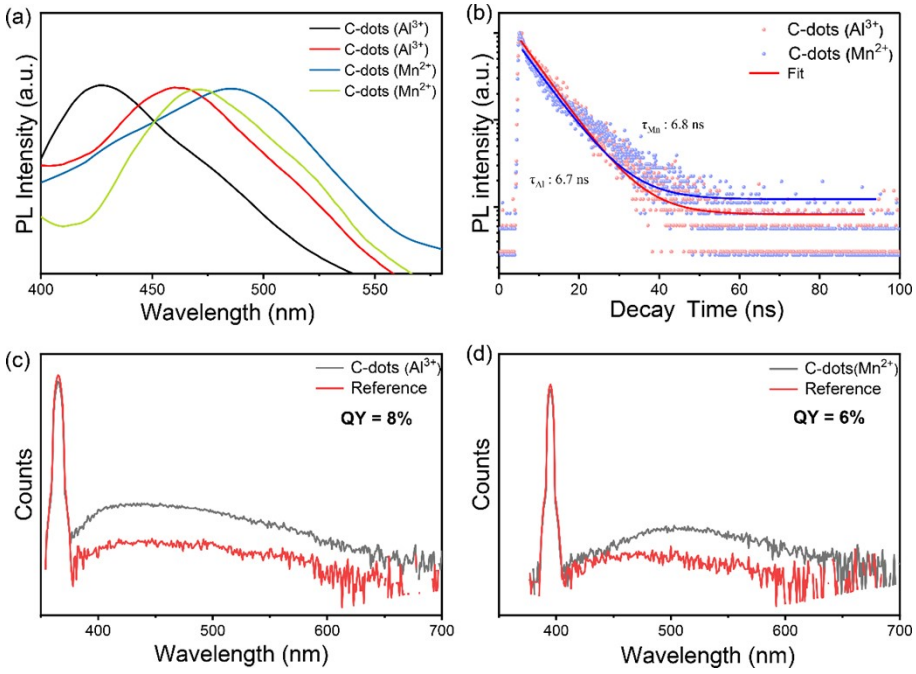

Figure S8. (a) PL spectra of the C-dots (Al^{3+}) and C-dots (Mn^{2+}) after printing. The excitation wavelength was set at 365 nm (black and blue) or 395 nm (red and light green). (b) The fluorescence decay curves of the C-dots (Al^{3+}) and C-dots (Mn^{2+}) after printing. (c) QYs of the C-dots (Al^{3+}) and C-dots (Mn^{2+}) after printing, excited at 375 nm. (c) QYs of the C-dots (Al^{3+}) after printing at 375 nm. (d) QYs of the C-dots (Mn^{2+}) after printing, excited at 375 nm.

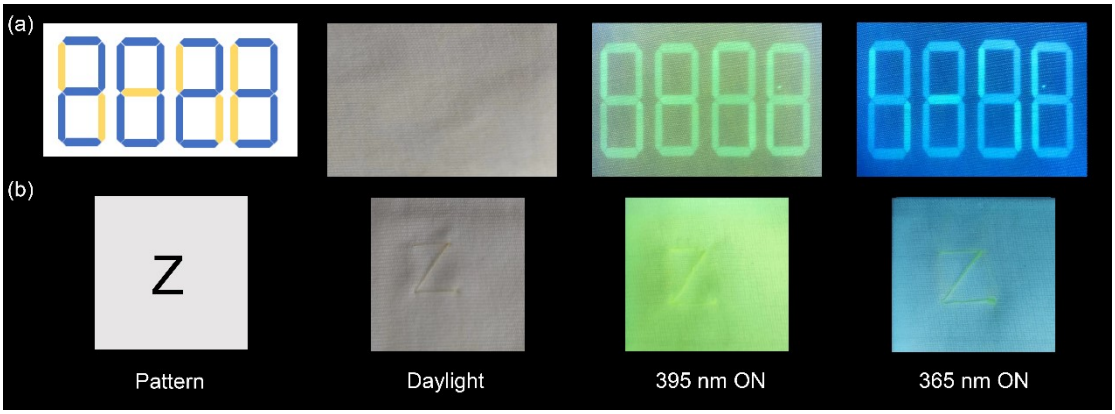

Figure S9. (a) The designed and printed anti-counterfeiting patterns on cotton upon room lighting and illumination of 395 nm and 365 nm. (b) The designed, dyed anti-counterfeiting fibers and cotton under room lighting, illumination of 395 nm and 365 nm.

3. Tables

Table S1 a: Content of various elements of the C-dots (Mn^{2+}) from XPS.

Sample	Relative contents			
	C	N	O	Mn
C-dots (Mn^{2+})	56.10%	8.41%	33.53%	2.28%

Table S1 b: Content of various elements of the C-dots (Sr^{2+}) from XPS.

Sample	Relative contents			
	C	N	O	Sr
C-dots (Sr^{2+})	53.57%	8.19%	36.18%	2.06%

Table S1 c: Content of various elements of the C-dots (Al^{3+}) from XPS.

Sample	Relative contents			
	C	N	O	Al
C-dots (Al^{3+})	51.22%	5.96%	31.93%	2.16%

Table S1 d: Content of various elements of the C-dots (In^{3+}) from XPS.

Sample	Relative contents			
	C	N	O	In
C-dots (In^{3+})	58.28%	6.15%	33.79%	1.78%

Table S1 e: Content of various elements of the C-dots (Ga^{3+}) from XPS.

Sample	Relative contents			
	C	N	O	Ga
C-dots (Ga^{3+})	54.13%	6.74%	37.38%	1.75%

Table S2: Research summary of metal ions doped or capped C-dots.

M-C-dots	**Synthesis approach**	**Precursors**	**QY**	**ref**
Zn-C-dots	Microwave digestion	$ZnSO_4$, ethylene diamine	14.26%	[1]
Zn-C-dots	One-step microwave-aided pyrolysis	citric acid, branched PEI_{25k}, and different zinc salts	60%	[2]
Mn-C-dots	Solvothermal Method	citric acid, urea, manganese acetate, toluene	68.6%	[3]
Mg-C-dots	Microwave- aided	hen feather, MgSO4	9.23%	[4]
Cu-C-dots	One-pot hydrothermal method	glucose, $CuSO_4·5H_2O$	39.1%	[5]
Al-C-dots	One-pot hydrothermal approach	Durian shell, urea, $Al(NO_3)_3·9H_2O$,	28.7%	[6]
Al-C-dots	Solvothermal method	Ophenylenediamine, N, N-dimethylformamide	1.99%	[7]
Ga-C-dots	one-step sonochemical synthesis	Polyethylene glycol-400 (99.998%), metallic gallium	1.8%	[8]
Fe-C-dots	Electrochemical oxidation	1,10-phenanthroline, $FeCl_3·6H_2O$	7.5%	[9]
Mn-C-dots	Heating method	Citric acid, urea, $MnCO_3$	61%	This work

Note and references

1. Y. Zhu, Y. Lu, L. Shi and Y. Yang, *Microchem. J.*, 2020, **153**, 104517 .
2. A. Hasanzadeh, F. Radmanesh, E. S. Hosseini, I. Hashemzadeh, J. Kiani, H. Nourizadeh, M. Naseri, Y. Fatahi, F. Chegini, Z. Madjd, A. Beyzavi, P. S. Kowalski and M. Karimi, *Bioconjugate Chem.*, 2021, **32**, 1875-1887.
3. Y. Liu, D. Chao, L. Zhou, Y. Li, R. Deng and H. Zhang, *Carbon*, 2018, **135**, 253-259.
4. T. Liu, N. Li, J. X. Dong, H. Q. Luo and N. B. Li, *Sens. Actuators, B*, 2016, **231**, 147-153.
5. A. M. Mahmoud, M. M. El-Wekil, R. Ali, H. A. Batakoushy and R. Y. Shahin, *Microchim. Acta*, 2022, **189**, 183.
6. S. Jayaweera, K. Yin, X. Hu and W. J. Ng, *J. Fluoresc.*, 2019, **29**, 1291-1300.
7. K. Yuan, X. Zhang, X. Li, R. Qin, Y. Cheng, L. Li, X. Yang, X. Yu, Z. Lu and H. Liu, *Chem. Eng. J.*, 2020, **397**, 125487.
8. V. B. Kumar, R. Kumar, A. Gedanken and O. Shefi, *Ultrason. Sonochem.*, 2019, **52**, 205-213.
9. S. Sun, W. Bao, F. Yang, X. Yan, Y. Sun, G. Zhang, W. Yang and Y. Li, *Green Energy Environ.*, 2023, **8**, 141-150.